Materials Science-Poland, Vol. 28, No. 4, 2010

Impedance and modulus spectroscopy studies of $Ba_4SrSmTi_3V_7O_{30}$ ceramics

P.S. SAHOO[1], A. PANIGRAHI[2], S.K. PATRI[3], R.N.P. CHOUDHARY[3]*

[1]Department of Physics, Betnoti College Betnoti, Mayurbhanj, Orissa, India

[2]Department of Physics, D.N. College, Itanagar, Arunachal Pradesh, India

[3]Department of Physics & Meteorology, IIT, Kharagpur, 721302, India

Modulus and impedance spectroscopy studies on barium strontium samarium vanadate ($Ba_4SrSmTi_3V_7O_{30}$) were carried out, as functions of frequency (1 kHz–1 MHz) and temperature (31–500 °C). XRD analysis of $Ba_4SrSmTi_3V_7O_{30}$ ceramic revealed the formation of single phase compound in an orthorhombic structure. The Cole–Cole plots showed a non-Debye type of dielectric relaxation. The dc and ac analyses of $Ba_4SrSmTi_3V_7O_{30}$ reveal typical negative temperature coefficient of resistance (NTCR) behaviour. The electric modulus, which describes the dielectric relaxation of the compound, is fitted to the Kohlrausch exponential function. Modulus analysis suggests the existence of a hopping mechanism for the electrical transport processes of the material.

Keywords: *electrical properties; SEM; X-ray diffraction*

1. Introduction

Materials of tungsten bronze (TB) structure belong to an important family of dielectric materials. Extensive studies of some ferroelectric materials of the TB structural family exhibit the occurrence of high electric permittivity (ε) and low dielectric loss [1, 2] along with interesting ferroelectric, pyroelectric, piezoelectric, and nonlinear optical properties are useful for various devices such as transducers, actuators, capacitors, and ferroelectric random access memory devices [3–7]. Various ionic substitutions in TB structures play an important role in tailoring their physical properties [4–7]. A detailed literature survey shows that not much work has been reported on the said compound $Ba_4SrSmTi_3V_7O_{30}$ (BSSTV). The dielectric and electrical (ac conductivity) properties of BSSTV have already been reported elsewhere [8]. The present paper summarizes the impedance properties of the BSSTV compound.

*Corresponding author, e-mail: crnpfl@phy.iitkgp.ernet.in

2. Experimental

Preparation of the material. A polycrystalline sample of BSSTV was fabricated using a high temperature solid state reaction technique. High purity (99.9 %) powders of $BaCO_3$, $SrCO_3$, TiO_2, Sm_2O_3 (Sarabhai M. Chemicals Pvt. Ltd., India), and V_2O_5 (Koch Light Ltd., England) in stoichiometric proportion were weighed and thoroughly ground in an agate mortar to obtain a homogeneous mixture, and then calcined at 950 °C for 12 h. The calcined powder was cold pressed into cylindrical pellets 10 mm in diameter and 1–2 mm thick under the pressure of 5×10^6 N/m^2 using a hydraulic press. Polyvinyl alcohol (PVA) was used as a binder to reduce the brittleness of the pellets, which was burnt out during high temperature sintering. Then the pellets were sintered at 1000 °C for 12 h in an air atmosphere using an alumina crucible. The sintered pellets were polished with fine emery paper to make the surfaces flat and parallel. To study the electrical properties of the compound, the both flat surfaces of the pellets were electroded with air-drying conducting silver paste. After electroding, the pellets were dried at 150 °C for 4 h to remove moisture, if any, and then cooled to room temperature before taking any measurement.

Characterization of the material. X-ray diffraction (XRD) data were collected with a Rigaku X-ray powder diffractometer (model: Miniflex) in a wide range of the the Bragg angles ($20° \le 2\theta \le 80°$) with CuK$_\alpha$ (λ = 1.5405 Å). The surface morphology and energy dispersive X-ray spectra (quantitative elemental analysis) were recorded under a scanning electron microscope JEOL (model: JSM-5800F). The electrical properties (i.e., the impedance and modulus parameters) of BSSTV were studied using a computer-controlled LCR meter (PSM 1735, model: N 4L) in a wide frequency range (from 1 kHz to 1MHz) at the ac signal (amplitude) of 1 V, starting at room temperature (31 °C) and ranging up to 500 °C.

3. Results and discussion

3.1. Structural study

Sharp, single peaks of the XRD pattern (Fig. 1) confirmed the formation of a new compound. All the prominent peaks were indexed, and the lattice parameters were refined using the least-squares refinement subroutine of the computer program POWDMULT [9]. The best agreement between observed (obs) and calculated (cal) interplanar spacing (d) was found in the orthorhombic crystal system. However, a few small peaks in the XRD pattern were identified. The refined lattice parameters of BSSTV are: a = 10.8212 (14) Å, b = 8.4211(14) Å, c = 20.7605(14) Å (with the estimated standard deviation in parenthesis). The Scherrer equation [10] was used to calculate the crystallite/particle size of the sample. The average particle size of the material was found to be 21 nm.

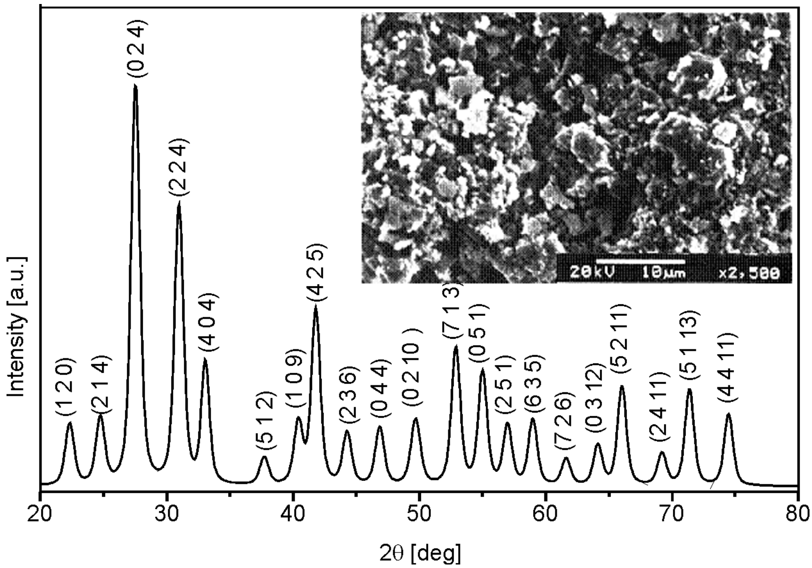

Fig. 1. Room temperature XRD pattern and SEM micrograph (inset) of $Ba_4SrSmTi_3V_7O_{30}$

The inset of Figure 1 shows the scanning electron micrograph of the BSSTV pellet at room temperature. The micrograph revealed the presence of uniformly and densely distributed nearly-spherical grains with a certain degree of porosity. The grain size (diameter of individual grains of ceramics) of the compound was found to be in the range of 1.2–2.2 μm. A similar type of microstructure was observed in many crystalline materials of this family [11–13].

3.2. Electrical analysis

The electrical behaviour of the system was studied over a wide range of frequencies and temperatures using an ac impedance spectrum (CIS) technique. The method enables us to separate real and imaginary components of the electrical parameters, and hence provides a true picture of the material properties. Using the CIS method, the grain and the grain boundary properties (having different time constants) of a polycrystalline material can usually be seen as two successive semicircles in the data representation.

3.2.1. Impedance spectrum analysis

Figure 2 shows the Nyquist plots (complex impedance spectrum) of BSSTV at some selected temperatures (200–500 °C). The spectrum is characterized by a single semicircular arc whose pattern of evolution changes upon increasing temperature which indicates the beginning of intergranular activities within the material sample with definite contributions from bulk (grain interior). In addition, the point of intercept of the arcs on the real axis has also been observed to shift towards the origin of the complex plane plot. This type of shift suggests a decrease in the resistive behaviour of the sample, assisted by the grain boundary conduction upon increasing temperature [14]. Such electrical phenomena in the material can appropriately be modelled in terms of an equivalent rc electrical circuit. This observation clearly indicates that the electrical properties of this material are largely controlled by its microstructure.

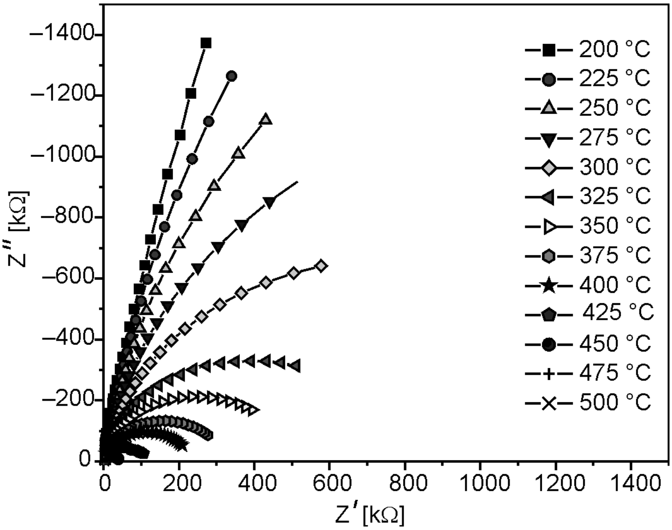

Fig. 2. Nyquist plot of $Ba_4SrSmTi_3V_7O_{30}$

Figure 3a shows the dependence of the imaginary part of the impedance (Z″) on the frequency (i.e., loss spectrum) at various temperatures (200–500 °C). The loss spectrum has some important features: (i) the appearance of a peak in the loss spectrum $Z''_{\max}$ (≥ 300 °C), (ii) typical peak broadening, and (iii) value of $Z''_{\max}$ decreases and shifts to higher frequencies as temperature increases. The asymmetric peak broadening suggests a spread of the relaxation time (i.e., the existence of a temperature dependent electrical relaxation phenomenon in the material) [15]. The peak heights are proportional to the bulk resistance (R_b), as expressed in the equation

$$Z'' = R_b \frac{\omega\tau}{1+\omega^2\tau^2}$$

where ω is angular frequency and τ – relaxation time. The relaxation process in the material may be due to the presence of immobile species/electrons at low temperatures and defects/vacancies at high temperatures. Figure 3b shows the variation of the real part of the impedance Z' as a function of the frequency at various temperatures (200–500 °C) for $Ba_4SrSmTi_3V_7O_{30}$. It is observed that Z' decreases as temperature increases, indicating a negative temperature coefficient of the resistance in the system.

The plateau region of the plot also indicates the presence of a relaxation process in the material.

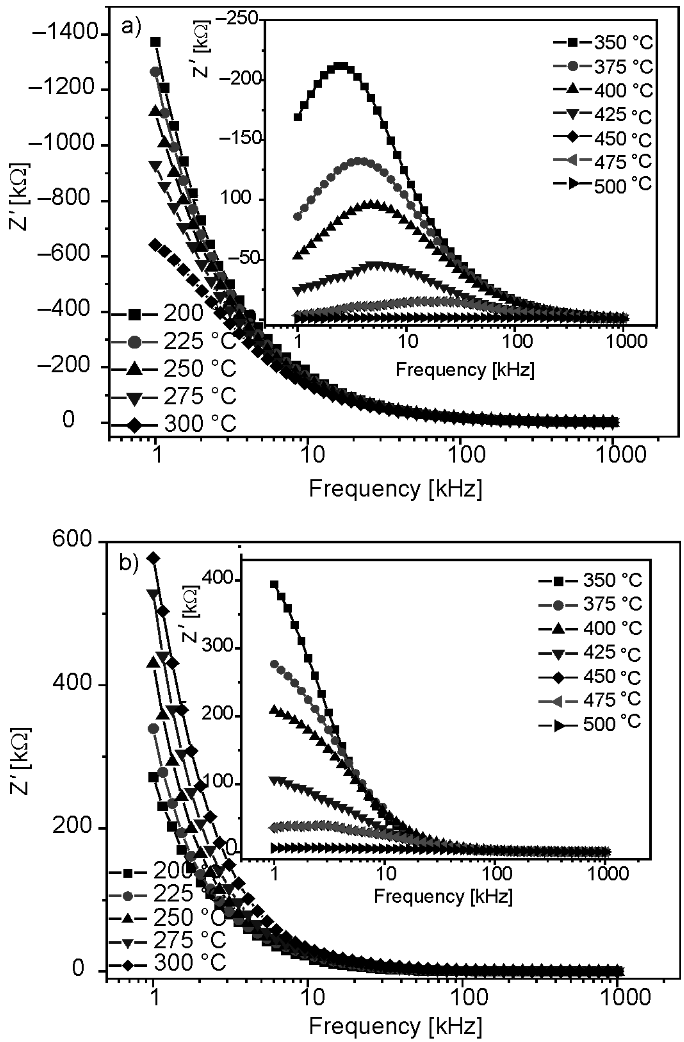

Fig. 3. Dependences of imaginary (Z'') (a) and real (Z') (b) parts of complex impedance of $Ba_4SrSmTi_3V_7O_{30}$ on the frequency

In the relaxation system, one can determine the most probable relaxation time (τ) from the position of the loss peak in the Z'' or M'' with frequency plots according to the dependence: $\tau = 1/\omega = 1/2\pi f_r$. The variation of relaxation time (τ) with the reciprocal temperature $1/T$ (K^{-1}) of BSSTV at high temperatures is shown in Fig. 4. The plot satisfies the Arrhenius equation, $\tau = \tau_0\exp(-E_a/K_BT)$, where the symbols have their usual meaning. The relaxation time is related to the thermally activated process. The activation energy of the compound, calculated from the above equation, is found to be

0.58 eV (Fig. 4). Based on the modulus plot, the dependence of τ on temperature is shown in the inset of Fig. 4. The value of the activation energy, obtained from the slope of the curve in the plot of logτ against 10^3T^{-1}, is found to be ~0.64 eV. It is clear that the activation energy of the compound (as calculated from the loss and modulus spectra) is nearly the same, and the relaxation process may be attributed to the same type of charge carrier.

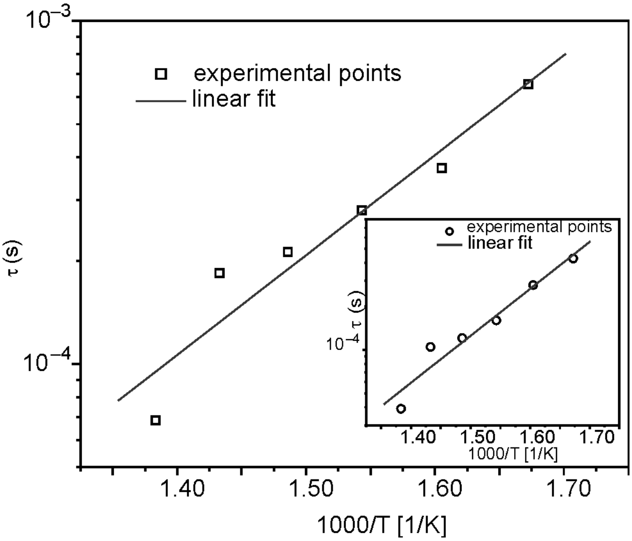

Fig. 4. Dependence of the relaxation time of $Ba_4SrSmTi_3V_7O_{30}$ on 1000/T calculated from the impedance spectrum (Z″ vs. frequency) and modulus spectrum (M'' vs. frequency) (inset)

3.2.2. Modulus spectrum analysis

In polycrystalline materials, the modulus of the impedance emphasizes the grain boundary conduction process, while bulk effects on frequency domain dominate in the electric modulus formalism. Modulus spectroscopy plots are particularly useful for separating spectral components of materials having similar resistances but different capacitances. The other advantage of the electric modulus formalism is that the electrode effect is suppressed. Due to the above reasons, complex electric modulus formalism has been opted. For the dielectric relaxation, studies have been carried out in the complex modulus M^* formalism. Variation of real (M') and imaginary (M'') parts of the electric modulus in function of frequency at various temperatures are shown in Fig. 5.

It is evident from Fig. 5a that for each temperature, M' reaches a constant value at higher frequencies. Also, at lower frequencies M' approaches 0, confirming the presence of an appreciable electrode and/or ionic polarization at the studied temperature. The value of M' increases from a low frequency towards high frequency limit and the dispersion shifts to higher frequencies as temperature increases. The dependences of M'' on frequency at various temperatures (Fig. 5b) reveals that as the frequency increases, M'' increases and attains a peak value at a particular frequency, for temperatures higher than 400 °C. The peak value of M'' at 450 °C is much lower compared with the corresponding peak value at other temperatures, indicating the transition temperature of the sample is ca. 450 °C. Above 450 °C, the value of M'' starts from the origin, increases proportionally with frequency, and attains a peak value at a particular frequency, and it subsequently decreases in inverse proportion to frequency. A similar trend has been found for all temperatures above 450 °C. However, at such temperatures, the peak values of M'' shift towards the higher frequency range as temperature increases.

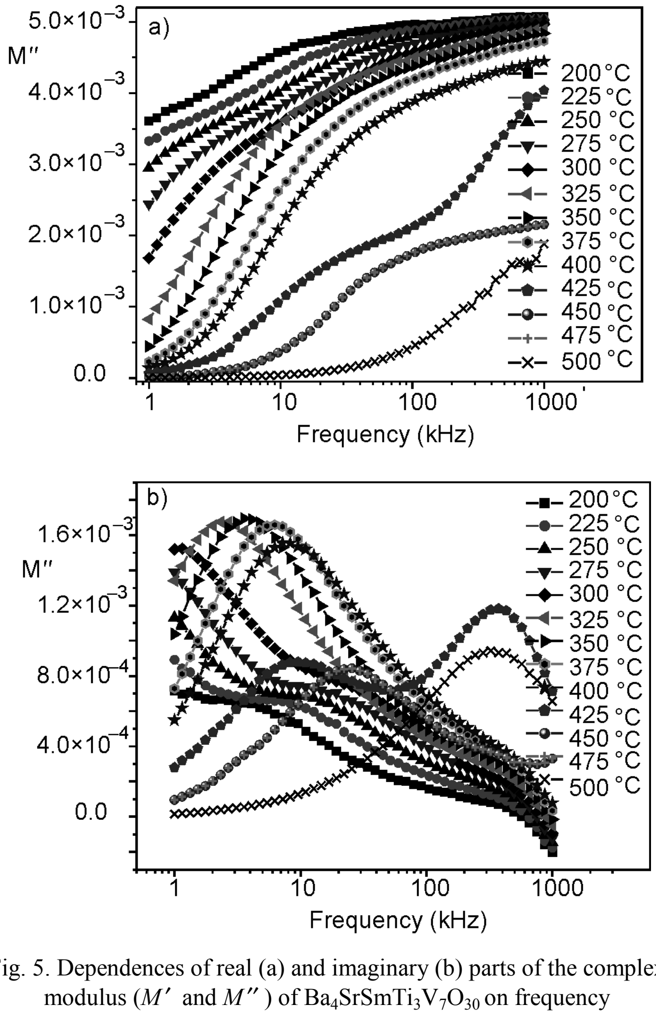

Fig. 5. Dependences of real (a) and imaginary (b) parts of the complex modulus (M' and M'') of $Ba_4SrSmTi_3V_7O_{30}$ on frequency

The complex modulus spectrum of BSSTV at higher temperatures (200–500 °C) is shown in Fig. 6. It is clear that the modulus plane shows two semicircles for temperatures higher than 300 °C; the intercept of the first (smallest) semicircle with the real axis indicates the total capacitance contributed by the grain, while the intercept of the second semicircle indicates the total capacitance contributed by the grain boundary. The modulus spectrum shows a marked change in its shape upon increasing temperature, suggesting a change in the value of capacitance of the material with temperature.

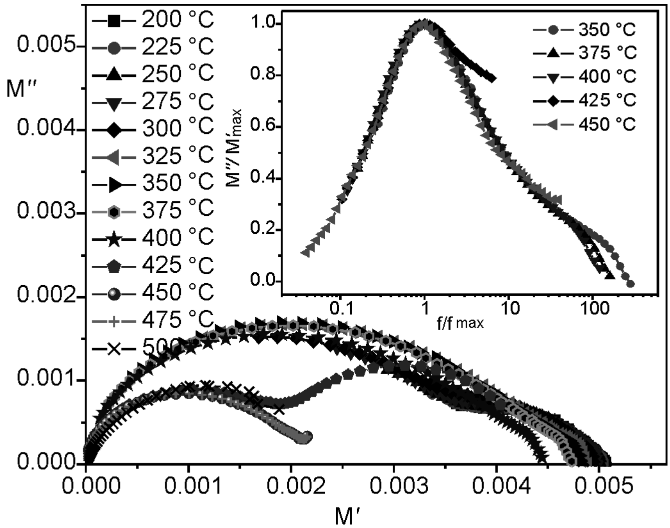

Fig. 6. Complex modulus spectrum (M'' vs. M') at various temperatures and dependence of M''/M''_{max} on f/f_{max} (inset) of $Ba_4SrSmTi_3V_7O_{30}$

The scaling behaviour of the sample was studied by plotting normalized parameters (i.e., M''/M''_{max} vs, $\log(f/f_{max})$, f_{max} is the frequency corresponding to M''_{max}) at various temperatures (inset of Fig. 6). The coincidence of all the curves of different temperatures into a single master curve indicates temperature independent dynamic processes [16]. This curve provides us with information about dielectric processes occurring in the material and the magnitude of mismatch between the peaks.

3.2.3. Conductivity analysis

The temperature–frequency dependence of electrical conductivity can be represented by an equation proposed by Jonscher [17]:

$$\sigma_{ac} = \sigma_{dc} + A\omega^n$$

where σ_{dc} conductivity is due to the excitation of electrons from a localized state to the conduction band, and $A\omega^n$ is the ac conductivity which consists of all dispersion phenomena. A is the frequency independent constant and n an exponent, $0 < n < 1$; both of these terms are temperature dependent. Figure 7 shows the dependence of ac conductivity on frequency at various temperatures. The conductivity pattern shows that it is strongly frequency dependent and obeys Jonscher's power relation, as given above.

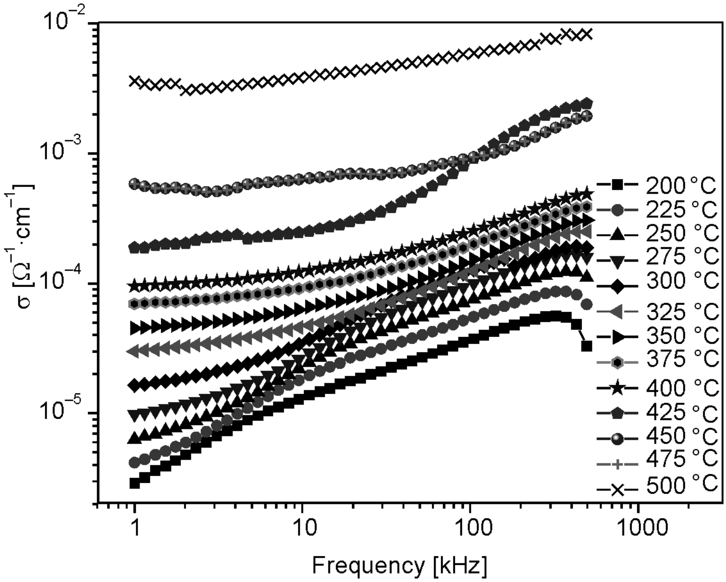

Fig. 7. Dependence of σ_{ac} of $Ba_4SrSmTi_3V_7O_{30}$on frequency

It clearly indicates that low and high frequency dispersive regions are separated by a change in slope at a particular frequency. The frequency at which a change in the slope occurs is called the hopping frequency.

4. Conclusions

$Ba_4SrSmTi_3V_7O_{30}$ was prepared by the mixed-oxide method. Preliminary X-ray analysis shows that the compound has an orthorhombic crystal structure at room temperature. Impedance spectroscopy was used to characterize the electrical properties of the material. The bulk effect was observed above 300 °C. The complex impedance plots show that the bulk resistance decreases upon increasing temperature, indicating the negative temperature coefficient of resistance behaviour of the sample. Analysis of the frequency dependence of ac conductivity shows that ac resistance follows the universal power law, as suggested by Jonscher. The conduction mechanism of the material may be due to the hopping of charge carriers.

References

[1] CHEN X.M., SUN Y.H., ZHENG X.H., J. Eur. Ceram. Soc., 23 (2003), 1571.

[2] FANG L., CHEN L., ZHANG H., DIAO C.L., YUAN R.Z., Mater. Lett., 58 (2004), 2654.

[3] NEURGAONKAR R.I., HALL W.F., OLIVER J.R., HO W.W., CORY W.K., Ferroelectrics, 87 (1998), 167.
[4] NEURGAONKAR R.R., CORY W.K., J. Opt. Soc. Am., 3 (1986), 276.
[5] NEURGAONKAR R.R., NELSON J.G., OLIVER J.R., Mater. Res. Bull., 25 (1990), 959.
[6] PANIGRAHI A., SINGH N.K., J. Mater. Sci. Lett., 18 (1999), 1579.
[7] RAJU M.R., CHOUDHARY R.N.P., J. Phys. Chem. Solids, 64 (2003), 847.
[8] SAHOO P.S., PANIGRAHI A., PATRI S.K., CHOUDHARY R.N.P., Mat. Lett., 63 (2009), 864.
[9] WU E., *POWD, An Interactive Powder Diffraction Data Interpretation and Indexing Program*, *Version 2.1*, School of Physical Sciences, Flinders Univ. of South Australia.
[10] CULLITY B.D., *Elements of X-ray Diffraction*, Addision-Wesley Publishing Co. Inc., 1978.
[11] BEHERA B., NAYAK P., CHOUDHARY R.N.P., Mater. Lett., 59 (2005), 3489.
[12] BEHERA B., NAYAK P., CHOUDHARY R. N. P., Mater. Chem. Phys., 100 (2006), 138.
[13] SAHOO P.S., PANIGRAHUA, PATRI S.K., CHOUDHARY R.N.P., Mod. Phys. Lett., B, 30 (2008), 2999.
[14] MACDONALD J.R., *Impedance Spectroscopy Emphasizing Solid Materials and Systems*, Wiley, New York, 1987.
[15] SCHERRER P., Göttinger Nachrichten, 2 (1918), 98.
[16] SAHA S., SINHA T.P., Phys. Rev. B. 65 (2002), 134103.
[17] JONSCHER A.K., Nature 267 (1977), 673.

Received 21 September 2008
Revised 7 August 2009